Arch. Metall. Mater. **69** (2024), 1, 73-76

DOI: https://doi.org/10.24425/amm.2024.147788

SRINIVASULU GRANDHI[1], KWANG-HYEOK JIN[1], MIN-SU KIM[2],
DONG-JOO YOON[3], SEUNG-HYO LEE[4*], MIN-SUK OH[1*]

IN-SITU WETTABILITY ANALYSIS OF Al COATING INFLUENCE ON HOT-DIP GALVANIZING PROPERTIES OF ADVANCED HIGH-STRENGTH STEELS

We investigated the influence of steel surface properties on the wettability of zinc (Zn). Our main objective is to address the selective oxidation of solute alloying elements and enhance the wetting behavior of Zn on advanced high strength steel (AHSS) by employing an aluminum (Al) interlayer through the physical vapor deposition technique. The deposition of an Al interlayer resulted in a decrease in contact angle and an increase in spread width as the molten Zn interacted with the Al interlay on the steel substrate. Importantly, the incorporation of an Al interlayer demonstrated a significant improvement in wettability by substantially increasing the work of adhesion compared to the uncoated AHSS substrate.

Keywords: Advanced high-strength steel (AHSS); selective oxidation; physical vapor deposition (PVD); contact angle; wetting

1. Introduction

Advanced high-strength steel (AHSS) has been developed to reduce the automobile body weight without compromising strength [1-3]. This contributes to environmental protection by improving fuel efficiency. Protecting an AHSS, like dual-phase (DP) steel, by galvanization (i.e., formation of Zn coating) remains challenging because solutes (like Mn and Si) in the steel could undergo selective oxidation during surface preparation before hot-dipping in galvanization lines [4-6]. Oxides on the substrate surface hinder the galvanization reaction, resulting in the formation of bare spots [5-7]. To avoid this issue, the DP steels have been precoated with Fe [8], Ni [9], Cu, and Cu-Sn [10] by electrodeposition or flash coating. In-situ contact angle measurements enable the analysis of the wettability by validating the surface preparation procedure and alloy coating parameters, making them a valuable approach in the hot-dip coating industry. Contact angle measurements by the sessile drop method are limited by contact angle deviations caused by the conservation of energy to vibrational energy [11]. The use of the current model alleviates the vibration problem. This study develops a physical vapor deposition (PVD) method to form an Al thin film interlayer on a DP steel substrate to eliminate the effect of selective surface oxidation before hot-dip galvanization. For comparison, a plain cold-rolled commercial quality (CQ) carbon steel with no/minimal solute effect is also tested. The effect of the steel surface on the coatability of Zn with and without an Al coating was investigated by measuring the contact angles during the coating process.

2. Experimental Methods

Two different substrates were tested in this study: (1) CQ steel with a composition of C-0.14, Mn-0.30, S-0.01, P-0.015, Si-0.025, Al-0.03, N-0.004, and Fe-99.476 (in wt%) and (2) DP steel with a composition of C-0.346, Si-0.25, Mn-1.29, and Cr-0.14 (in wt%); trace quantities of P, S, Ni, Mo, V, Ti, Al, Nb, B, and N; and Fe as the remainder. Based on the surface condition of the tested steel, the substrates were designated as as-received (CQ and DP) and Al-coated (ACQ and ADP). In the deposition process, a 99.95% pure Al pellet source was thermally evaporated (PVD) on to the steel substrates by varying current through a thermal evaporator (KVE-T400, VACUUM TECH, Korea). The chamber was maintained at a vacuum of 10^{-6} Torr. The Alpha-Step Stylus Profiler (D-500, KLA, CA,

[1] JEONBUK NATIONAL UNIVERSITY, DIVISION OF ADVANCED MATERIALS ENGINEERING AND RESEARCH CENTER FOR ADVANCED MATERIALS DEVELOPMENT, JEONJU, REPUBLIC OF KOREA
[2] KOREA INSTITUTE OF INDUSTRIAL TECHNOLOGY, GIMJE, REPUBLIC OF KOREA
[3] SUNCHON NATIONAL UNIVERSITY, CENTER FOR PRACTICAL USE OF RARE MATERIALS, SUNCHON, REPUBLIC OF KOREA
[4] KOREA MARITIME & OCEAN UNIVERSITY, DEPARTMENT OF OCEAN ADVANCED OF MATERIALS CONVERGENCE ENGINEERING, PUSAN, REPUBLIC OF KOREA

* Corresponding authors: misoh@jbnu.ac.kr, lsh@kmou.ac.kr

US) uses a moving probe to acquire Al-coating thickness with precision ranging from a few nanometers to several hundreds of micrometers. The contact angle of Zn with the steel substrates was measured using a high-temperature Contact Angle Analyzer (Phoenix HT-10, SEO, Suwon, South Korea). Zn was cut into cubes of 5 mm × 5 mm × 5 mm. The heating rate was maintained at 5°C/min until the temperature reached 600°C, in normal atmospheric conditions. All samples were held at 600°C for 45 min and then cooled to room temperature inside the furnace. The in-situ images of Zn melting on the steel substrate at different instances were captured at 1-s intervals using a high-speed camera. The spread width and contact angles were measured from the start of the melting of the Zn cube until the end of the holding time. Photographs of the substrate surface were used for visual inspection. The cross-sectional microstructure of the coated samples was observed using a field-emission scanning electron microscope (FE-SEM) (SUPRA 40VP, Carl Zeiss, MA, US) equipped with energy-dispersive X-ray spectroscopy (EDX) to examine the Zn-steel substrate interface.

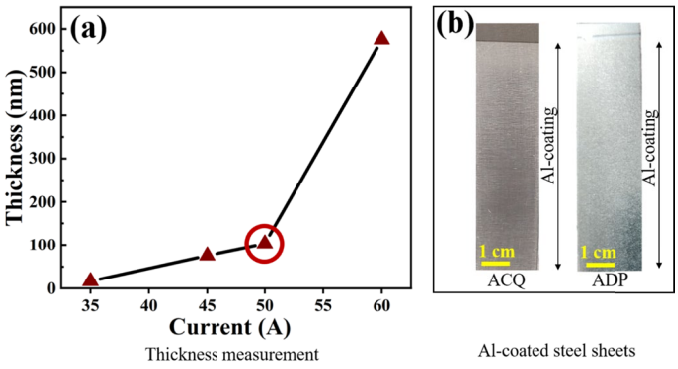

Fig. 1. (a) Thickness measurement of Al coating on steel substrate by Alpha-step; (b) Al-coated CQ and DP steels (designated as ACQ and ADP respectively)

3. Results and Discussion

The Al coating was deposited on steel substrates with currents of 35 A, 45 A, 50 A, and 60 A while keeping the deposition time constant at 5 min. The thickness of the Al coating was measured and plotted as shown in Fig. 1(a). A deposition thickness of approximately 100 nm was chosen (marked in Fig. 1(a)). The corresponding deposition current and time were kept constant at 50 A and 5 minutes, respectively, for deposition on CQ and DP steels. The surface of the Al-coated CQ and DP steel sheets is shown in Fig. 1(b).

The shapes of the Zn cube at the initial stage, start of melting, and after the holding time are shown in Fig. 2(a)(i), 2(a)(ii), and 2(a)(iii), respectively. A comparison of the Al-coated and bare samples revealed an increase in the spread width of Zn that continued until the end of the experiment for the former but not for the latter. Qualitatively, we inferred that the contact angle of Zn with the substrate changes; specifically, it decreased for Al-coated samples but hardly changed for bare samples. The samples were removed after cooling to room temperature. As shown in Fig. 2(b), solidified Zn adhered to the surface of the Al-coated sheet, whereas no Zn was detected on the surface of the bare sheet. The wetting and non-wetting behaviors of the melting Zn are schematically shown in Fig. 2(c)(i) and 2(c)(ii), respectively.

The wetting behavior was further analyzed by calculating the spread width and contact angle from the captured experimental images. A comparison of the plots of the spread width (Fig. 3(a) and contact angle (Fig. 3(b)) indicated that the increase in the spread width alone does not confirm the wettability. Although the spread width of Zn on CQ and DP steel substrates initially increased, it became stagnant during the holding time; simultaneously, no decrease was seen in the contact angle. By contrast, in the case of ACQ and ADP steel substrates, an increase in the spread width resulted in a decrease in the contact angle, indicating their interdependence on the wettability of Zn on the steel substrate.

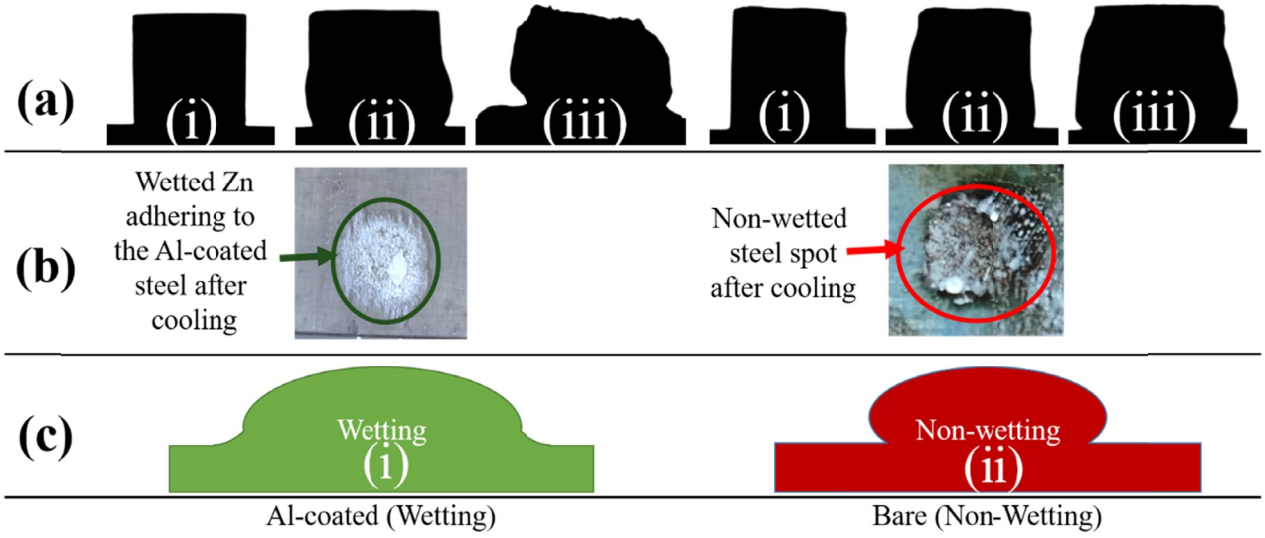

Fig. 2. (a) Shape of Zn cube: (i) initial, (ii) start of melting, and (iii) end of holding time; (b) photographs of sample surfaces: wetted and non-wetted steel surfaces after cooling; (c) schematic of wetting and non-wetting samples

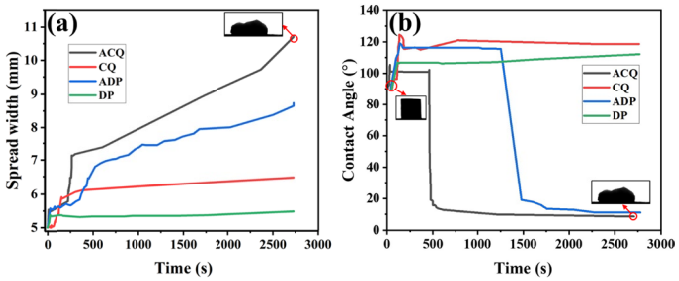

Fig. 3. (a) Spread width of Zn cube with time for different steel substrates. (b) Contact angle of Zn with different steel substrates

The major driving force for increased wetting can be understood from the following calculations of the interfacial energy [12]:

$$\sigma_{sg} = \sigma_{lg}\left(\sqrt{\left(1+\sin^2\theta\right)}+\cos\theta\right) \quad (1)$$

$$\sigma_{sl} = \sigma_{lg}\left(\sqrt{\left(1+\sin^2\theta\right)}-\cos\theta\right) \quad (2)$$

$$W_a = \sigma_{sg} + \sigma_{lg} - \sigma_{sl} \quad (3)$$

where σ_{sg} is the surface energy of the substrate; σ_{lg}, the surface energy of molten Zn; W_a, the work of adhesion (i.e., energy released during wetting); and θ, the instantaneous contact angle. As the molten zinc was maintained at the same temperature for all samples, the surface energy of the liquid (σ_{lg}) was considered constant (σ_{Zn}), and therefore, σ_{sg} (Eq. (1)) and W_a (Eq. (3)) were calculated in terms of σ_{Zn}. The surface energy is due to the energy of the incomplete bonds on the material surface [13]. The interfacial surface energy of the substrate (σ_{sg}) for Al-coated steels (ACQ and ADP) was higher than that for uncoated steels (CQ and DP). The increased surface energy of the steel substrate indicated that the Al coating cleaned oxides and Al atoms solidified on the nascent steel substrate [14]. Owing to the surface cleaning provided by Al deposition, the high-energy surface of the steel substrate readily reacted with Zn, resulting in improved wetting. Further, owing to the presence of Fe oxide compounds on CQ and DP steels, the surface energy was low and interactions with liquid Zn were prevented; thus, no wetting was observed.

The molten Zn-steel substrate interfacial energy (σ_{sl}) (Eq. (2)) (Fig. 4(b)) and contact angle (Fig. 3(b)) reduced for Al-coated steels but was almost the same for bare steel substrates. This indicated that hot molten Zn reaching the steel substrate through the Al-coating layer might have led to the interdiffusion of Fe and Zn atoms and thereby improved the wettability. W_a (inset in Fig. 4(a) as it followed similar trend with time) increased for Al-coated steels as the surface energy of steel (σ_{sg}) increased and that of molten Zn (σ_{sl}) decreased [15,16], thereby increasing the wettability. As almost no energy change occurred in bare CQ and DP steels, W_a was constant, and therefore, no wetting was observed. The solid_solubility of Al in Zn increases with temperature and simultaneous possible inhibition layer formation through Fe-Al alloying might have improved the wettability.

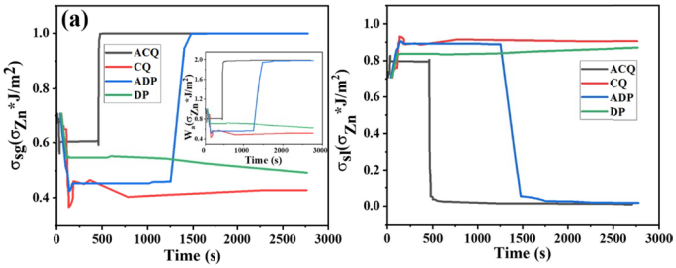

Fig. 4. (a) Interfacial surface energy of ACQ, ADP increased with wetting of zinc; work of adhesion increased with wetting on ACQ and ADP; (b) interfacial energy between molten zinc and steel substrates of ACQ, ADP decreased with wetting

As wetting was evident only for ACQ and ADP steel substrates, they were subjected to cross-sectional microstructural observation using SEM (Fig. 5). Secondary electron images of

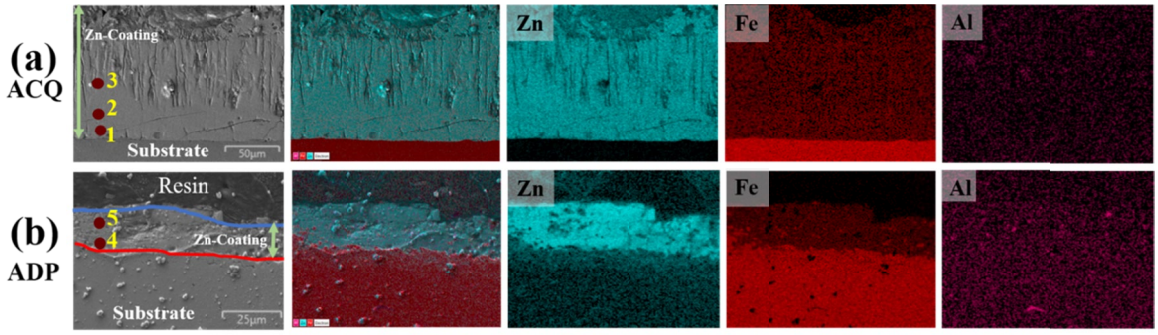

EDS	Fe (wt. %)	Zn (wt. %)	Al (wt. %)
1	17.12	82.85	0.02
2	11.21	88.77	0.01
3	7.91	92.07	0.01
4	24.71	75.26	0.02
5	13.40	86.56	0.03

Fig. 5. (a) ACQ: secondary electron image, respective phase maps with Fe/Zn/Al mixed, EDX analysis and individual phase maps of Zn and Fe. (b) ADP: secondary electron image, EDX analysis and respective phase maps with Fe/Zn/Al mixed, and individual phase maps of Zn, Fe and Al

ACQ and ADP revealed an intact interface between the steel substrate and solidified Zn without crack formation, indicating metallurgical bond formation. The EDX phase maps show the distribution of Fe and Zn. Due to the significant time provided for wetting reactions to occur, no trace of Al was detectable at the interface, as evidenced by the Al EDX phase map and quantitative analysis. The marked EDX locations representative of different regions where EDX analysis was conducted, and mean values of the results obtained from each respective region are presented. Therefore, the provision of an Al-interlayer helped successfully form a Zn coating on AHSS (i.e., DP steel in the current study).

4. Conclusions

This study investigated the effect of the steel substrate surface on the wettability of Zn. Zn did not wet the bare steel surface owing to the presence of oxides. The introduction of a thin Al coating as an interlayer improved the wettability Zn of both CQ and DP steels by provision of a nascent steel surface enhanced reactivity with molten metal, and thereby improved bonding through increased work of adhesion. The combined influence possible formation of Fe-Al inhibition layer and increased solid solubility of Al in Zn might have played a significant role in improving the wettability.

Acknowledgements

This work was supported by the [National Research Foundation of Korea (NRF)] grant funded by the Korea Government (Ministry of Science and ICT) [No. 2022R1A2C1008972]. This work was also supported by the Technology Innovation Program (20016850) funded by the Ministry of Trade, Industry & Energy (MOTIE, Korea). This work was also supported in part by the Technology Development Program (S3160560) funded by the Ministry of SMEs and Startups (MSS, Korea).

REFERENCES

[1] Y.S. Jin, La Metall. Ital. **6**, 43-48 (2011).
[2] J.I. Yoon, H.H. Lee, H.K. Park, K. Ameyama, H.S. Kim, J. Korean Powder Metall. Inst. **24**, 128-132 (2017).
[3] D. Kim, Y. Han, M. Moon, H. Oh, Corros. Sci. Technol. **10**, 1-6 (2009).
[4] R. Khondker, a. Mertens, J.R. McDermid, Mater. Sci. Eng. A. **463**, 157-165 (2007).
[5] H. Liu, F. Li, W. Shi, S. Swaminathan, Y. He, M. Rohwerder, L. Li, Surf. Coatings Technol. **206**, 3428-3436 (2012).
[6] L. Cho, E.J. Seo, G.S. Jung, D.W. Suh, B.C. De Cooman, Metall. Mater. Trans. A. **47**, 1705-1719 (2016).
[7] S. Alibeigi, R. Kavitha, R.J. Meguerian, J.R. McDermid, Acta Mater. **59**, 3537-3549 (2011).
[8] M.G. Walunj, G.K. Mandal, R.K. Ranjan, R. Pais, S.K. Mishra, T. Venugopalan, L.C. Pathak, Surf. Coatings Technol. **422**, 127573 (2021).
[9] D. Pradhan, M. Dutta, T. Venugopalan, J. Mater. Eng. Perform. **25**, 4996-5006 (2016).
[10] M. Manna, M. Dutta, Surf. Coatings Technol. **251**, 29-37 (2014).
[11] S. Shimada, Y. Takada, J. Lee, T. Tanaka, ISIJ Int. **48**, 1246-1250 (2008).
[12] T. Liu, R. Ma, Y. Fan, A. Du, X. Zhao, M. Wen, X. Cao, Surf. Coatings Technol. **337**, 270-278 (2018).
[13] https://www.ossila.com/pages/a-guide-to-surface-energy
[14] M. Lee, I. Bae, Y. Kwak, K. Moon, Curr. Appl. Phys. **12**, S2-S6 (2012).
[15] B.K. Cheng, B. Naccarato, K.J. Kim, A. Kumar, Int. J. Heat Mass Transf. **102**, 154-161 (2016).
[16] M.M.R.M.M. Affandi, M. Tripathy, A.B.A. Majeed, J. Mol. Liq. **240**, 340-344 (2017).